Volume 25
Number 14
14 April 2023
Pages 2013–2166

CrystEngComm

rsc.li/crystengcomm

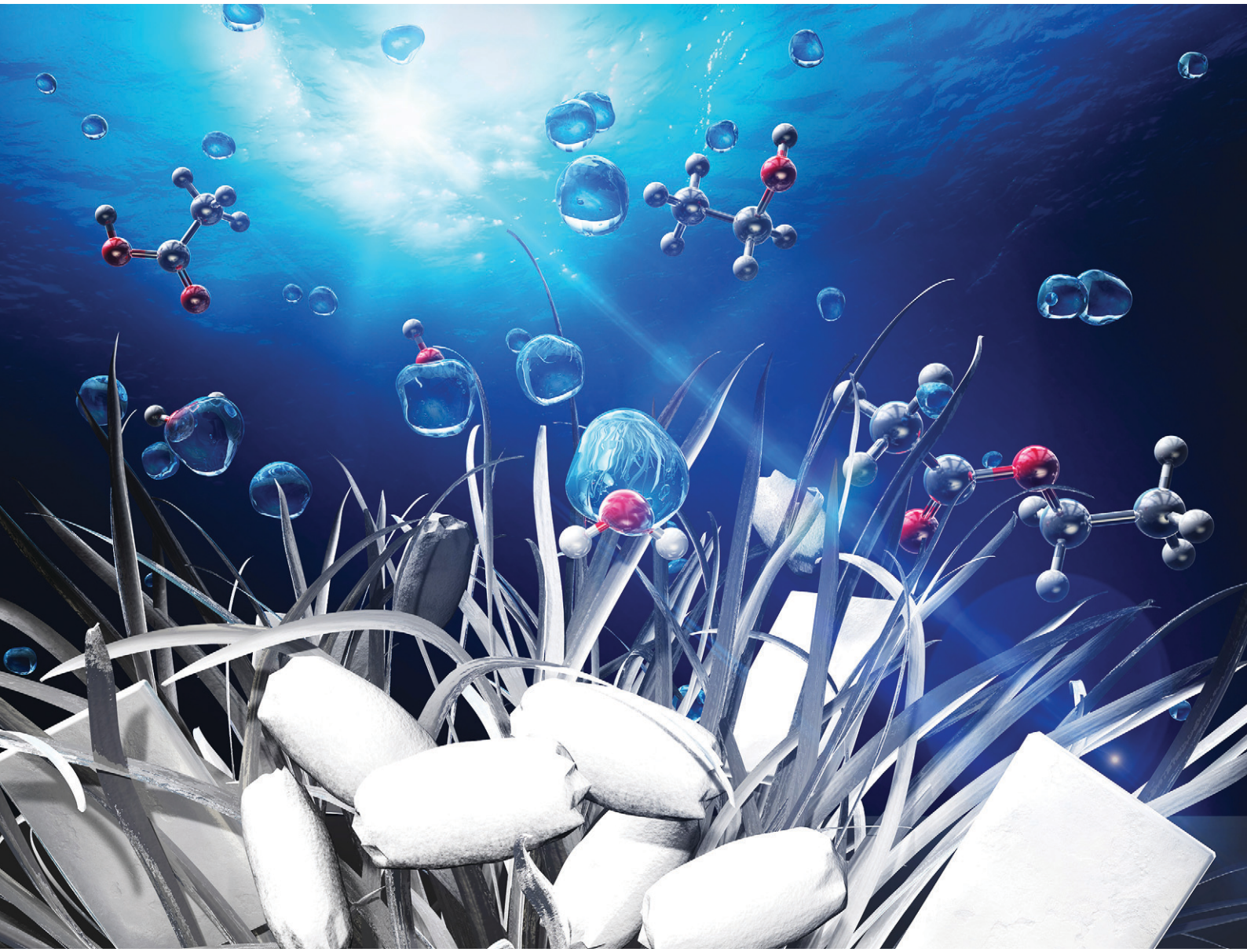

ISSN 1466-8033

ROYAL SOCIETY OF CHEMISTRY

COMMUNICATION

Tomoyo Goto *et al.*

Simultaneous synthesis of hydroxyapatite fibres and β-tricalcium phosphate particles *via* a water controlled-release solvothermal process

CrystEngComm

ROYAL SOCIETY OF CHEMISTRY

COMMUNICATION

View Article Online
View Journal | View Issue

Check for updates

Cite this: *CrystEngComm*, 2023, **25**, 2021

Received 28th December 2022,
Accepted 16th February 2023

DOI: 10.1039/d2ce01703b

rsc.li/crystengcomm

Simultaneous synthesis of hydroxyapatite fibres and β-tricalcium phosphate particles *via* a water controlled-release solvothermal process†

Tomoyo Goto, *[ab] Shu Yin, [cd] Yusuke Asakura, [e] Sung Hun Cho[a] and Tohru Sekino [a]

Fibrous hydroxyapatite was synthesised from α-tricalcium phosphate in ethanol and acetic acid solutions *via* a water controlled-release solvothermal process (WCRSP). Rice-like particles of β-tricalcium phosphate were formed by adjusting the solvent conditions. Results indicated that the water concentration achieved in the WCRSP is essential for determining crystal phase and morphology.

Introduction

Hydroxyapatite (HAp; $Ca_{10}(PO_4)_6(OH)_2$), whose chemical composition is similar to that of the inorganic component of bone, is well known as an artificial bone filler material owing to its high osteoconductivity.[1] The adsorption and ion-exchange properties of HAp and related calcium phosphate have enabled their use as adsorbents for chromatographic media of proteins[2,3] or adsorbents for pollutant removal.[4,5] Previous studies suggest that these properties of HAp depend on crystallographic properties such as crystal phase and morphology.[6–10] Therefore, the morphological control of HAp-based functional materials is a powerful tool for enhancing the chemical properties of their surface in the medical or environmental fields. Based on these research backgrounds, liquid-based synthesis is a suitable synthetic method. The hydrothermal or solvothermal method, which is a liquid-based synthesis method, is excellent for the precipitation and crystal growth of inorganic compounds with varied crystal morphology and an automorphic form.[11] The morphology and composition of HAp are also easily altered in the hydrothermal method *via* starting materials and treatment conditions such as temperature, solvents, and additives.[6,9–13] In general, nucleation and crystal growth behaviour in the liquid phase is strongly affected by the supersaturation degree and its change rate. In addition, the presence of 'water' in the liquid phase is key for the nucleation and crystal growth of HAp, and the contribution of water is particularly large on HAp formation, as can be also inferred from the chemical composition. For instance, solvent control or reactivity of raw materials with water results in large morphological changes.[13,14] The controlled release of water in the solvent is estimated to have a significant effect on HAp formation under hydrothermal or solvothermal conditions. However, the crystal growth behaviour of HAp in an environment with extremely limited water in the organic solvent has not been reported extensively.

Therefore, in this study, HAp synthesis was attempted *via* a water controlled-release solvothermal process (WCRSP) utilising the esterification reaction of alcohol and carboxylic acid. Yin *et al.* reported the synthesis of homogeneous nanoparticles such as Cs_xWO_3 nanorods *via* the WCRSP.[15–17] Because the amount of water supplied is suppressed, the WCRSP can be performed to synthesise various nanomaterials under highly supersaturated conditions, and this method is also expected to be effective for the synthesis of nanosized HAp. For this investigation, α-tricalcium phosphate (α-TCP) was selected as a starting material. α-TCP is a high-solubility product and is used as a self-curing cement of calcium phosphate for bone repair as it reacts quickly and forms HAp.[18] Additionally, it is advantageous as a starting material for the synthesis of HAp because HAp crystals of various morphologies can be obtained *via* the hydrolysis reaction of α-TCP owing to its variable dissolution

[a] *SANKEN (The Institute of Scientific and Industrial Research), Osaka University, 8-1 Mihogaoka, Ibaraki, Osaka 567-0047, Japan. E-mail: goto@sanken.osaka-u.ac.jp*
[b] *Institute for Advanced Co-Creation Studies, Osaka University, 1-1 Yamadaoka, Suita, Osaka 565-0871, Japan*
[c] *Institute of Multidisciplinary Research for Advanced Materials (IMRAM), Tohoku University, 2-1-1, Katahira, Aoba-ku, Sendai 980-0877, Japan*
[d] *Advanced Institute for Materials Research (WPI-AIMR), Tohoku University, 2-1-1, Katahira, Aoba-ku, Sendai 980-0877, Japan*
[e] *Kagami Memorial Research Institute for Materials Science and Technology, Waseda University, 2-8-26 Nishiwaseda, Shinjuku-ku, Tokyo 169-0051, Japan*

† Electronic supplementary information (ESI) available: Characterization, FT-IR spectra, TEM-EDX images, SEM images, XRD patterns, fraction of integrated intensity, N_2 sorption isotherms, element composition, and starting materials of solvothermal treatment. See DOI: **https://doi.org/10.1039/d2ce01703b**

depending on the synthesis conditions.[13,14,19–22] The effects of synthesis conditions such as the solvent, temperature, and stirring in the WCRSP on the formation behaviour and crystal morphology of HAp synthesised from α-TCP were investigated. To the best of our knowledge, there is no precedent for a method that uses a non-aqueous solvent as a starting point for the solvothermal synthesis of HAp, and therefore this study is significant for the development of HAp-related materials on both basic and applied research.

Experimental

α-TCP powder ($Ca_3(PO_4)_2$, Taihei Chemical Industrial Co., Ltd., Osaka, Japan), used as a starting material, was dispersed into a mixed solution of ethanol (99.5%, Wako Pure Chemical Industries, Ltd., Osaka, Japan) and acetic acid (99.7%, Wako Pure Chemical Industries, Ltd., Osaka, Japan), and then the sample was mixed using a magnetic stirrer for a few minutes at room temperature. The mixture samples (20 mL) were added in a 50 mL polytetrafluoroethylene (PTFE) vessel and sealed in an autoclave (SAN-AI Kagaku Co. Ltd., Nagoya, Japan). Then, the autoclaves were treated with or without stirring for up to 24 h in a dry oven (DRM 320DD, Advantec Toyo Kaisha, Ltd., Tokyo, Japan) at 120 °C, 150 °C, and 180 °C, and the ethanol : acetic acid mixture ratios were 5 : 15, 10 : 10, 12 : 8, and 15 : 5 (volume ratios), respectively. These are denoted E05A15, E10A10, E12A08, and E15A05 in order. Subsequently, the products were washed with ethanol and removed *via* suction filtration. The products were dried in an oven at 40 °C. Simultaneously, α-TCP powder, as a control sample, was also treated using single solvents of water, ethanol (E20A00), and acetic acid (E00A20). Detailed conditions for each sample are summarised in Table S1.† The products were characterised *via* physicochemical methods that have been extensively described in the ESI.†

Results and discussion

The reactivity of α-TCP against single solvents under solvothermal conditions was investigated without stirring at 150 °C for 24 h. After the solvothermal treatment in water, the α-TCP phase (PDF no. 01-070-0364) was completely transformed into HAp single phase (PDF no. 00-009-0432), and the formation of fine needle- or plate-shaped crystals was observed, as shown in Fig. 1(a) and S1(a).† Additionally, the dissolution of α-TCP and three-phase formation, *i.e.*, HAp, β-TCP (PDF no. 00-009-0169) and dicalcium phosphate anhydrous (DCPA) (PDF no. 01-077-0128) were observed in acetic acid conditions (E00A20). Large plate-like, fine needle-shaped, and fine nanocrystals were formed as they were mixed (Fig. 1(a) and S1(b)†). In contrast, α-TCP did not react in ethanol conditions (E20A00), and crystal phase and morphology were maintained (Fig. 1(a) and S1(c)†). Fig. 1(b) and 2 show the crystal phase and morphology of products after the hydrothermal treatment using ethanol–acetic acid solutions with constant stirring. In the E10A10 sample with a

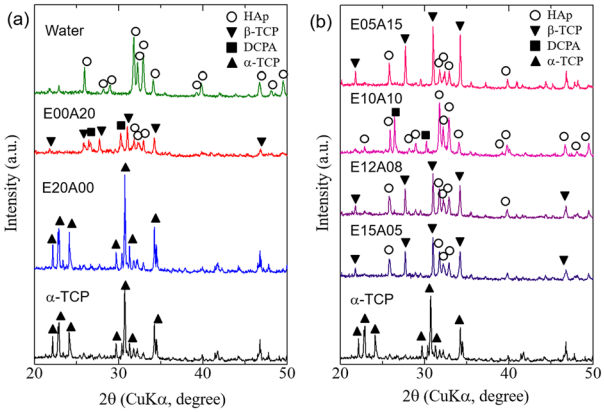

Fig. 1 X-ray diffraction (XRD) patterns of products after solvothermal treatment at 150 °C for 24 h, using various solvents: (a) water, acetic acid (E00A20), ethanol (E20A00), and (b) ethanol and acetic acid mixtures.

nearly equimolar ratio of ethanol and acetic acid, HAp and DCPA were detected (Fig. 1(b)), and long whisker-like or fibrous crystals were observed. A large plate-shaped crystal was also partially present (Fig. 2(b) and (f)). In the case of E05A15, E12A08, and E15A05 samples, HAp and β-TCP phases were detected, and fibrous or needle-shaped crystals extending on the particles were observed (Fig. 2(a), (c) and (d)). Additionally, rice-like particles with peculiar morphology were observed in E05A15 samples (Fig. 2(e)). The results of the FT-IR analysis (Fig. S2†) of samples presented in XRD results (Fig. 1) showed good agreement. The typical HAp pattern was observed in samples treated with water,[23] while the samples treated with ethanol displayed only the P–O and O–P–O bonds of α-TCP used as the starting material. In contrast, the sample

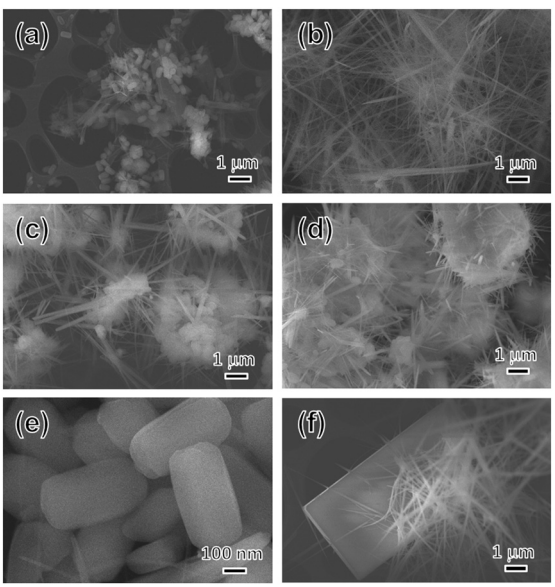

Fig. 2 SEM images of products after solvothermal treatment at 150 °C for 24 h, using an ethanol–acetic acid system. (a) E05A15, (b) E10A10, (c) E12A08, (d) E15A05, (e) E05A15, and (f) E10A10.

solvothermally treated with acetic acid (E00A20) showed the presence of C═O and C–H bond.[24] However, the typical peak of a carboxyl group (C═O stretching) at approximately 1770 cm^{-1} was not detected in this sample which can be attributed to the absorption of a small amount of acetic acid by the sample. Phosphate bonds derived from calcium phosphates, and hydroxyl bonds were detected in the samples of mixed solvent; for example, the bond corresponding to the hydroxyl group of HAp was detected at 638 cm^{-1} and 3570 cm^{-1} in the E10A10 sample. The hydrogen phosphate bond at 865 cm^{-1} was also detected, indicating the presence of calcium-deficient HAp or DCPA in the samples.[23] Additionally, the C═O and C–H bonds were observed with an increase in the content of acetic acid in the solvent derived from the acetic acid or ethyl acetate, indicating that the solvent molecule could be easily adsorbed on the surface of calcium phosphate with a higher concentration of acetic acid in the solvent. Although no single-phase samples were obtained, elemental analysis was conducted to investigate the crystals of each type of morphology *via* transmission electron microscope (TEM) and Energy Dispersive X-ray Spectroscopy (EDX) analysis, as shown in Fig. S3 and Table S2.† The needle-shaped, rice-like, and plate-shaped crystals showed a lower Ca/P ratio which were 0.64, 0.77 and 0.74, respectively. The Ca/P atomic ratio of HAp, β-TCP, and DCPA (as stoichiometric composition) are 1.67, 1.5, and 1.0 respectively. The detected Ca/P ratio is much lower than the theoretical value; therefore, the determination of the crystal phase of different crystals from the Ca/P ratio is difficult by EDX analysis.

To further analyse the structure of each crystal, TEM images and selected area electron diffraction (SAED) pattern for fibrous crystals (Fig. 3(a)–(c)), rice-like particles (Fig. 3(d)–(f)), and large plate crystals (Fig. 3(g)–(i)), were obtained. The long needle-shaped or fibrous crystals were well consistent with the unit cell parameter of the HAp phase (PDF no. 00-009-0432), as shown in Fig. 3(a), and HAp crystal growing along the *c*-axis (Fig. 3(b) and (c)). Notably, the SAED pattern of the rice-like particle, shown in Fig. 3(f), indicated a periodic pattern of bright spots without a ring pattern or overlapping spots; therefore, the rice-like particle was determined to be a well-crystallised single crystal (Fig. 3(d) and (e)). The unit cell parameter of the rice-like crystal was consistent with the β-TCP of the rhombohedral of the *R3c* space group (PDF no. 01-070-2065). Additionally, the SAED pattern of the rectangular plate-shaped crystal could not be observed owing to its high thickness (Fig. 3(g)). Therefore, a high-resolution TEM (HRTEM) image and FFT pattern of the plate-shaped crystal were obtained (Fig. 3(h) and (i)). From these results, the crystal structure of the rectangular plate-shaped crystals was determined to be of DCPA phase. This result is also consistent with the studies suggesting that DCPA has a large plate-like shape.[25] In addition, the effects of treatment temperature on the crystal phase and morphology were also investigated. Fig. S4† shows the XRD patterns and SEM images of products after the solvothermal treatment at various temperatures using E10A10 with constant stirring. HAp phase was detected in all samples, and DCPA formation increased with increasing temperature. Additionally, the β-TCP phase was also detected at 120 °C (Fig. S4(a)†). Fibrous and long needle-

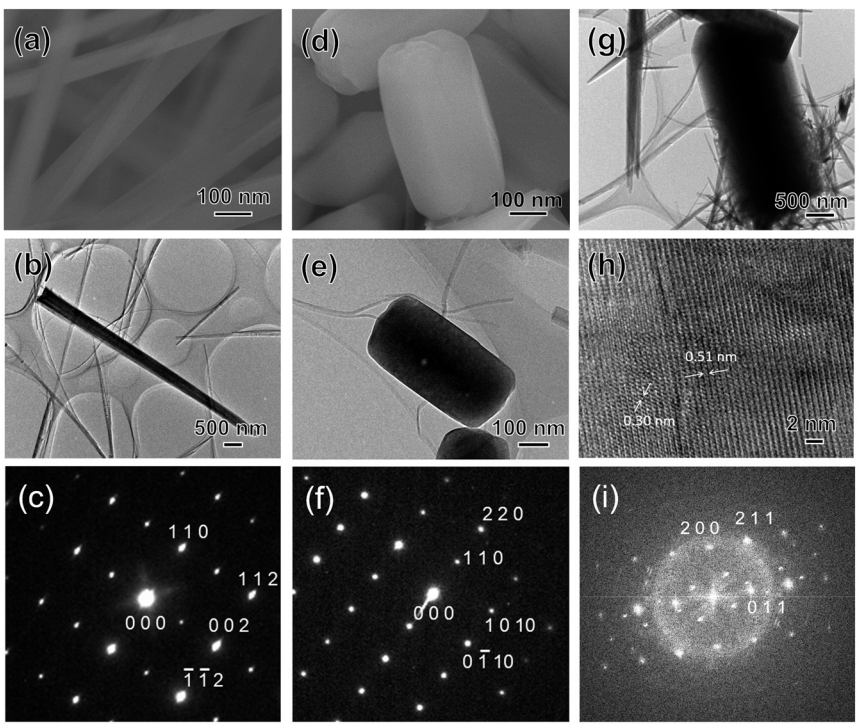

Fig. 3 SEM, TEM, HRTEM images, SAED, and FFT patterns of products: (a–c) fibrous HAp crystals, (d–f) rice-like β-TCP crystals, and (g–i) plate-shaped DCPA crystals.

shaped crystals were observed in the SEM images of all samples, and the length of fibrous crystal at 150 °C was observed to be the longest among all samples. Large plate-shaped crystals were also observed in the samples at 180 °C that seemed to be DCPA phase (Fig. S4(e)†). Fig. S5† shows the N_2 adsorption–desorption isotherms and surface area of these samples. Fig. S5(d)† shows that with increasing the treatment temperature, the surface area of the samples slightly increased, and indicates the morphological changes in crystals. In addition, α-TCP was treated with the WCRSP without stirring at various temperatures to investigate the effect of stirring conditions. At 120 °C, HAp formation was small, and α-TCP was almost transformed into β-phase in all samples (Fig. S6†). HAp formation also increased with an increase in the temperature and the peaks of DCPA were observed as the formation of HAp in the E10A10 sample increased. Fig. S7† shows the fraction of integrated intensity against the treatment temperature that was calculated using the XRD patterns (shown in Fig. S6†) of HAp, β-TCP, and DCPA phases in the samples. The HAp phase of the samples increased with increasing the treatment temperature. The fraction of HAp formation (approximately 80%) in the E10A10 sample was the highest at 150 °C; furthermore, the formation of HAp was found to decrease (approximately 60%) at higher temperatures. Compared with the results of the reaction with stirring (Fig. S4†), the formation ratio of β-TCP tended to increase at 120 °C regardless of the solvent type, and stirring promotes the formation of HAp in all samples. Especially, α-TCP was detected in the E15A05 sample without stirring, indicating the remains of the α-TCP phase *via* the surface formation of HAp due to a reaction with water molecules of the solvent.

Synthesis of HAp *via* hydrothermal or solvothermal methods has been widely studied in biomedical and environmental fields.[1–5] Water molecules are needed for the synthesis of HAp crystals because of the presence of hydroxide ions in the chemical structure of HAp. In many cases, HAp synthesis has been performed in a water-based solvent or a steam atmosphere. Therefore, this study presents the first report on the synthesis of HAp from a non-aqueous solvent using WCRSP, indicating the contribution of water molecules in the synthetic reactions. Fig. 4 shows the summary of the formation of fibrous HAp and rice-like β-TCP particles in the solvent conditions produced *via* the WCRSP. The WCRSP forms the water molecules *via* an esterification reaction, as shown in reaction (1).[15–17]

$$C_2H_5OH + CH_3COOH \rightarrow CH_3COOC_2H_5 + H_2O \quad (1)$$

Released water molecules react with α-TCP particles and the HAp phase is formed on the particles. Simultaneously, solution pH decreases with an increase in the HAp formation, as shown in reaction (2).

$$10Ca_3(PO_4)_2 + 6H_2O \rightarrow 3Ca_{10}(PO_4)_6(OH)_2 + 2PO_4^{3-} + 6H^+ \quad (2)$$

E10A10 samples showed a nearly equimolar reaction, and 0.17 mol of water is estimate to form *via* the esterification

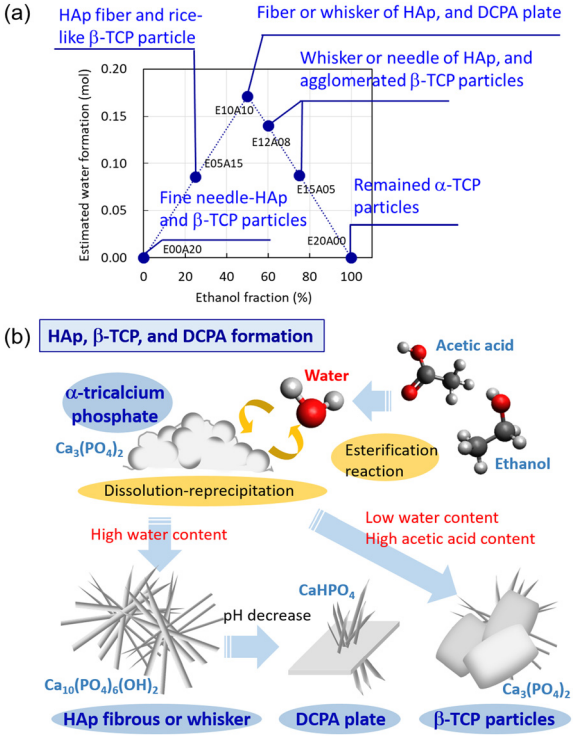

Fig. 4 (a) Relationships between the ethanol fraction of solvent, water formation, and crystal phase and morphology of products, and (b) summary of formation of calcium phosphate phases and the conditions of WCRSP.

reaction of the WCRSP. In contrast, water molecules reacted with 0.81 mmol of α-TCP, and solution pH around α-TCP particles decreased by the formation of H^+. DCPA phase was easily formed with HAp formation in this reaction because of the most stable phase changes from HAp to DCPA under acidic conditions (pH ≤ 4) in the solubility diagrams of calcium orthophosphates.[26] In contrast, the β-TCP phase is difficult to achieve in the aqueous solution in general, because β-TCP easily reacts with water, resulting in the formation of HAp as well as α-TCP.[26,27] However, the partial β-TCP formation was often observed in the solvothermal treatment of α-TCP using alcohol,[10,20] because the β-TCP phase could be a metastable phase in the reaction.[20] Therefore, the results indicate that the amount of water formed *via* WCSRP greatly affects the crystal phase formed from α-TCP. In terms of crystal morphology, fibrous or whisker-like HAp crystals, growing along the *c*-axis, was formed *via* the WCRSP. HAp was easily grown with the needle-like, whisker-like, or fibrous morphology in solvothermal or hydrothermal conditions,[10,28–30] and the growth rate of HAp along the *c*-axis was large. Moreover, the length of the needle-shaped crystal of HAp increased with increasing the treatment temperature, as shown in Fig. S4.† This morphology change was also observed when the reaction rate was suppressed by the addition of alcohol;[10,20] therefore, it can be concluded that the changes in the dissolution–reprecipitation rate of the solvent affect the crystal length

and width of HAp. In contrast, the formation of rice-like particles of β-TCP was observed especially in the E05A15 sample of solvothermal treatment. Although a few studies have reported the synthesis of β-TCP *via* hydrothermal or solvothermal method,[31,32] by the previous our work, as mentioned above, it is presumed that β-TCP is likely to form under conditions where dissolution and precipitation are difficult to occur when α-TCP was used as a raw material. In addition, it almost no reports on the morphological control using liquid-based methods are present in the literature. The α-TCP phase remained in ethanol (E20A00), however, α-TCP was reacted and dissolved in acetic acid (E00A20) *via* solvothermal synthesis, as shown in Fig. 1 and 2. These results indicate that rice-like β-TCP was achieved *via* dissolution–reprecipitation reaction, not phase transformation from α-TCP. The possible reason for this unique structure is that acetic acid or ethyl acetate formed were selectively adsorbed, which contributed to the crystal growth of β-TCP. These findings indicate the possibility of controlling the β-TCP morphology *via* the liquid phase method and the significance on the explication of formation mechanism of β-TCP as well. In the present study, biphasic products were formed in most of the samples. Biphasic products consisting of HAp and β-TCP are also used as a research object for medical application, and therefore this method is expected to be useful. In addition, these results also demonstrate the need for more water reactivity control, pH adjustment, and clarifying the contribution of ester to obtain single phases with unique morphologies by this method.

Conclusions

The non-aqueous synthesis of fibrous HAp and rice-like β-TCP particles from α-TCP *via* the WCRSP was reported. The crystal phase and morphology of calcium orthophosphates were largely affected by changes in the water content formed by the esterification reaction of ethanol and acetic acid and the resulting degree of high supersaturation. The results indicated that fibrous HAp easily grows along the direction of the *c*-axis in these conditions. By contrast, the unique rice-like β-TCP was formed as a metastable phase using the synthesis method presented herein, and this morphology was presumed to be an effect of the absorption of an organic molecule during crystal growth *via* the WCRSP. This study suggests that the crystal morphology of HAp and β-TCP can be controlled by focusing on the water supply process in the solvothermal treatment.

Author contributions

TG conceived and designed the study, and performed sample preparation, characterisation, and data analysis. SY and TS designed the experiment methods. YA and SHC considered the analysis results. All authors worked on drafts of the manuscript and approved the final report.

Conflicts of interest

There are no conflicts to declare.

Acknowledgements

This work was financially supported by the Japan Society for the Promotion of Science (JSPS) KAKENHI (grant numbers: JP20K12220 and JP22H04543) and 'Dynamic Alliance for Open Innovation Bridging Human, Environment and Materials' in the 'Network Joint Research Center for Materials and Devices' (MEXT, Japan). TEM and FTIR analyses were performed at the Comprehensive Analysis Center, SANKEN, at Osaka University, Japan. We thank Mr. Y. Murakami (Osaka Univ., Japan) for their technical support in TEM, HRTEM, SAED, and TEM-EDX observations.

Notes and references

1 J. Park, *Bioceramics: Properties, Characterizations and Applications*, Springer, New York, 1998.
2 T. Kawasaki, *J. Chromatogr.*, 1991, **544**, 147.
3 K. Ohta, H. Monma and S. Takahashi, *J. Biomed. Mater. Res.*, 2001, **55**, 409.
4 M. Ibrahim, M. Labaki, J.-M. Giraudon and J.-F. Lamonier, *J. Hazard. Mater.*, 2020, **383**, 121139.
5 I. L. Balasooriya, J. Chen, S. M. K. Gedara, Y. Han and M. N. Wickramaratne, *Nanomaterials*, 2022, **12**, 2324.
6 G. Kawachi, T. Watanabe, S.-I. Ogata, M. Kamitakahara and C. Ohtsuki, *J. Ceram. Soc. Jpn.*, 2009, **117**, 847.
7 K. Kandori, A. Fudo and T. Ishikawa, *Colloids Surf., B*, 2002, **24**, 145.
8 S. Hirakura, T. Kobayashi, S. Ono, Y. Oaki and H. Imai, *Colloids Surf., B*, 2010, **79**, 131.
9 T. Goto and K. Sasaki, *Powder Technol.*, 2016, **292**, 314.
10 T. Goto, S. H. Cho, C. Ohtsuki and T. Sekino, *J. Environ. Chem. Eng.*, 2021, **9**, 105738.
11 K. Yanagisawa, *J. Ceram. Soc. Jpn.*, 2005, **113**, 565.
12 M. Yoshimura and H. Suda, in *Hydroxyapatite and Related Materials*, ed. P. W. Brown and B. Constantz, CRC Press, Boca Raton, FL, 1994, p. 4572.
13 T. Goto, *J. Ceram. Soc. Jpn.*, 2022, **130**, 163.
14 T. Goto, I. Y. Kim, K. Kikuta and C. Ohtsuki, *J. Ceram. Soc. Jpn.*, 2012, **120**, 131.
15 C. Guo, S. Yin, P. Zhang, M. Yan, K. Adachi, T. Chonan and T. Sato, *J. Mater. Chem.*, 2010, **20**, 8227.
16 S. Yin, *J. Ceram. Soc. Jpn.*, 2015, **123**, 823.
17 S. Yin and T. Hasegawa, *KONA*, 2023, **40**, 94.
18 R. G. Carrodeguas and S. De Aza, *Acta Biomater.*, 2011, **7**, 3536.
19 M. Kamitakahara, C. Ohtsuki, G. Kawachi, D. Wang and K. Ioku, *J. Ceram. Soc. Jpn.*, 2008, **116**, 6.
20 T. Goto, I. Y. Kim, K. Kikuta and C. Ohtsuki, *Ceram. Int.*, 2012, **38**, 1003.
21 X. Liu, K. Lin and J. Chang, *CrystEngComm*, 2011, **13**, 1959.

22 R. Karalkeviciene, E. Raudonyte-Svirbutaviciene, J. Gaidukevic, A. Zarkov and A. Kareiva, *Crystals*, 2022, **12**, 253.
23 S. Koutsopoulos, *J. Biomed. Mater. Res.*, 2002, **62**, 600.
24 M. T. Colomer, *J. Sol-Gel Sci. Technol.*, 2013, **67**, 135.
25 K. Suchanek, A. Bartkowiak, M. Perzanowski and M. Marszałek, *Sci. Rep.*, 2018, **8**, 15408.
26 J. C. Elliot, *Structure and Chemistry of the Apatites and Other Calcium Orthophosphates*, Elsevier, Amsterdam, 1994.
27 S. V. Dorozhkin, *J. Mater. Sci.*, 2007, **42**, 1061.
28 M. Yoshimura, H. Suda, K. Okamaoto and K. Ioku, *J. Mater. Sci.*, 1994, **29**, 3399.
29 J. Liu, X. Ye, H. Wang, M. Zhu, B. Wang and H. Yan, *Ceram. Int.*, 2003, **29**, 629.
30 I. S. Neira, Y. V. Kolen'ko, O. I. Lebedev, G. V. Tendeloo, H. S. Gupta, F. Guitián and M. Yoshimura, *Cryst. Growth Des.*, 2009, **9**, 466.
31 T. Toyama, K. Nakashima and T. Yasue, *J. Ceram. Soc. Jpn.*, 2002, **110**, 716.
32 G. Zhu, Y. Hu, Y. Yang, R. Zhao and R. Tang, *RSC Adv.*, 2015, **5**, 23958.